

CONF-9507160--2

SAND95-1752C

Proposed for presentation at the 28<sup>th</sup> Annual International Metallographic Society (IMS) Convention, an Affiliate Society of ASM International, July 23-26, 1995, Albuquerque, NM.

## INSPECTION OF CHEMICALLY ROUGHENED COPPER SURFACES USING OPTICAL INTERFEROMETRY AND SCANNING ELECTRON MICROSCOPY: ESTABLISHING A CORRELATION BETWEEN SURFACE MORPHOLOGY AND SOLDERABILITY

J. O. Stevenson, F. M. Hosking, T. R. Guilinger, F. G. Yost, and N. R. Sorensen

Sandia National Laboratories  
Albuquerque, New Mexico, 87185

RECEIVED

AUG 17 1995

OSTI

### Abstract

Sandia National Laboratories has established a Cooperative Research and Development Agreement with consortium members of the National Center for Manufacturing Sciences (NCMS) to develop fundamental generic technology in printed wiring board materials and surface finishes. We are investigating the effects of surface roughness on the wettability and solderability behavior of several types of copper board finishes to gain insight into surface morphologies that lead to improved solderability. In this paper, we present optical interferometry and scanning electron microscopy results for a variety of chemically-etched copper substrates. Initial testing on six chemical etches demonstrate that surface roughness can be greatly enhanced through chemical etching. Noticeable improvements in solder wettability were observed to accompany increases in roughness.

ROUGH SURFACES AND THEIR IMPLICATIONS FOR WETTABILITY have been studied by many researchers.<sup>[1-10]</sup> These studies established the importance of surface roughness in wetting phenomena. Work by Wenzel described surface conditions necessary for wetting.<sup>[1]</sup> Wenzel developed a relationship showing that increases in roughness produce decreased contact angles between wetting liquid and solid substrate. This early result has been investigated for years in an effort to understand wetting behavior on rough surfaces.

Romero & Yost<sup>[9]</sup> and Yost *et al.*<sup>[10]</sup> have determined that an additional driving force exists for wetting on rough or grooved surfaces, namely, flow into open channel capillaries. Liquid solder flows into the open channels by capillary action. Solder flow within these V-shaped grooves is dependent on the orientation and physical dimensions of the grooves. Electroplated and electroless-plated copper inherently possess some degree of open capillary roughness that encourages solder flow. It was our intent to enhance this roughness using chemical etches. By producing V-shaped grooves through chemical etching, we would have an opportunity to further study the wetting behavior of rough surfaces and perhaps enhance the manufacturability of solder interconnects for electronic assemblies.

As the number of interconnections and the operating speed of electronic devices have increased, the fundamental limits of existing printed wiring board (PWB) manufacturing technologies are becoming increasingly apparent. PWB technology has been challenged to keep pace with advances in interconnection density and operating speed. The domestic PWB industry also faces serious foreign competition from large, well-financed firms.

An industry-wide desire for improved solder joint manufacturability and reliability has provided the impetus for our efforts to produce "engineered" rough surfaces. The following targets have been identified as potential impact areas:

- Enhanced solder flow on fine pitch circuits
- Equivalent Sn/Pb solderability with Pb-free solders
- Overcome plated-through-hole "weak knee"
- Improved adhesion of metallic or organic coatings

As finer pitches (i. e. finer spacing between patterned lines) continue to be *de rigueur*, the need to ensure complete coverage of solder pads continues to escalate. Incomplete solder coverage is a problem that grows more serious with decreasing pitch. The "defective" region becomes a much larger percentage of the total solder pad area as pitch decreases. The effort to maximize board real estate by increasing density and going to ever finer pitches will certainly exacerbate the potential for problems.

Conventional Sn/Pb solders exhibit very good area of spread and low contact angles. However, recent efforts to reduce or eliminate Pb have produced solders with low area of spread and alarmingly high contact angles. Wenzel's equations encourage us to view surface roughness as a process variable that can be utilized to improve wettability by increasing area of spread and decreasing contact angle.

Surface roughness has also been successfully used to improve the plated-through-hole "weak-knee" problem observed in many PWB applications.<sup>[11]</sup> The thinning of solder coatings at convex areas (i.e. plated-through-holes) on the PWB often leads to diminished solderability in these locations. During the solder dipping or reflow process, molten solder may not flow around these edges, producing the so-called "weak knee". Solder joints at the weak knee are often very poor and are the source of numerous failures.

## **DISCLAIMER**

This report was prepared as an account of work sponsored by an agency of the United States Government. Neither the United States Government nor any agency thereof, nor any of their employees, make any warranty, express or implied, or assumes any legal liability or responsibility for the accuracy, completeness, or usefulness of any information, apparatus, product, or process disclosed, or represents that its use would not infringe privately owned rights. Reference herein to any specific commercial product, process, or service by trade name, trademark, manufacturer, or otherwise does not necessarily constitute or imply its endorsement, recommendation, or favoring by the United States Government or any agency thereof. The views and opinions of authors expressed herein do not necessarily state or reflect those of the United States Government or any agency thereof.

## **DISCLAIMER**

**Portions of this document may be illegible  
in electronic image products. Images are  
produced from the best available original  
document.**

The adhesion of copper with other metallic and organic PWB materials may be improved by increasing surface roughness. Large increases in surface area promote simple adhesion by providing increased contact sites. While increased surface areas are generally desirable for promoting adhesion, high surface areas in copper create corrosion concerns due to water condensation in pores and crevices. Rough copper surfaces may require protection with an organic solderability preservative (OSP) coating[12].

Surface roughness may be enhanced in a variety of ways. Electroplating can increase the surface roughness of copper substrates.[10] Electrochemical etching also has the potential for increasing surface roughness. A literature search uncovered numerous chemical etches for copper.[11, 13-30] The referenced applications are myriad and do not necessarily seek increased surface roughness. Applications include manufacture of semiconductor devices and printed circuit boards, dissimilar materials joining, microjoining, diffusion welding, and ultrasonic welding. Table 1 presents a sampling of chemicals that have been used to etch copper.

Table 1. Sampling of chemicals used to etch copper.

Ammonia Solutions	Nitric Acid Solutions
$(\text{NH}_4)_2\text{S}_2\text{O}_8$	dilute $\text{HNO}_3$
$\text{NH}_4\text{CuCl}_3$	$\text{HNO}_3, \text{HNO}_2$
$\text{NH}_4\text{Cl}, (\text{NH}_4)_3\text{PO}_4, \text{Cu}^+$	✓ $\text{HNO}_3, \text{Cu}(\text{NO}_3)_2$
$[\text{CuNH}_3]\text{Cl}_2, \text{NH}_3, \text{NaClO}_2$	✓ $\text{HNO}_3, \text{H}_2\text{SO}_4$
$[\text{CuNH}_3]\text{SO}_4, \text{NH}_3, \text{S}_2\text{O}_8$	$\text{HNO}_3, \text{CH}_3\text{SO}_3\text{H}$
$[\text{Cu}(\text{NH}_3)_4]\text{SO}_4, \text{NH}_3, \text{Cl}^-$	
Sulfuric Acid Solutions	Chloride Solutions
✓ $\text{H}_2\text{SO}_4, \text{H}_2\text{O}_2$	$\text{FeCl}_3$
$\text{H}_2\text{SO}_4, \text{H}_2\text{O}_2, \text{NH}_3$	✓ $\text{FeCl}_3, \text{HCl}$
✓ $\text{Na}_2\text{SO}_4, \text{H}_2\text{SO}_4, \text{H}_2\text{O}_2$	$\text{CuCl}_2$
$\text{Na}_2\text{S}_2\text{O}_8$	✓ $\text{CuCl}_2, \text{H}_2\text{O}_2, \text{HCl}$
$\text{H}_2\text{S}_2\text{O}_8$ , halide	
	✓ initial test suite

Table 2. Chemical composition of etching solutions.

<b><math>\text{H}_2\text{SO}_4/\text{H}_2\text{O}_2</math></b> - Prepare 20 vol% $\text{H}_2\text{SO}_4$ stock solution (1 part 95-98% $\text{H}_2\text{SO}_4$ and 4 parts $\text{H}_2\text{O}$ ). Add 14 mls $\text{H}_2\text{O}_2$ per liter of stock solution.
<b><math>\text{Na}_2\text{SO}_4/\text{H}_2\text{SO}_4/\text{H}_2\text{O}_2</math></b> - Use 20 vol% $\text{H}_2\text{SO}_4$ stock solution. Add 14 mls $\text{H}_2\text{O}_2$ and 253 g $\text{Na}_2\text{SO}_4$ per liter of stock solution.
<b><math>\text{HNO}_3/\text{Cu}(\text{NO}_3)_2</math></b> - Prepare 50 vol% $\text{HNO}_3$ stock solution (equal parts 69-71% $\text{HNO}_3$ and $\text{H}_2\text{O}$ ). Add 253 g $\text{Cu}(\text{NO}_3)_2$ per liter of stock solution.
<b><math>\text{HNO}_3/\text{H}_2\text{SO}_4</math></b> - Prepare 2 parts 95-98% $\text{H}_2\text{SO}_4$ , 2 parts 69-71% $\text{HNO}_3$ , and 1 part $\text{H}_2\text{O}$ solution.
<b><math>\text{FeCl}_3/\text{HCl}</math></b> - Prepare 50 vol% $\text{HCl}$ stock solution (equal parts 36-38% $\text{HCl}$ and $\text{H}_2\text{O}$ ). Add 253 g $\text{FeCl}_3$ per liter of stock solution.
<b><math>\text{CuCl}_2/\text{H}_2\text{O}_2/\text{HCl}</math></b> - Use 50 vol% $\text{HCl}$ stock solution. Add 14 mls $\text{H}_2\text{O}_2$ and 253 g $\text{CuCl}_2$ per liter of stock solution.

## Materials & Experimental Procedure

We selected six etches to evaluate from the list in Table 1, two each from Sulfuric Acid Solutions, Nitric Acid Solutions, and Chloride Solutions. The initial test suite of six etches has been denoted with check marks in Table 1. The six etching solutions were formulated as shown in Table 2.

Two different types of copper substrate materials were investigated in this study: electroless copper (EL) and electroplated copper (EP). EL and EP copper possess inherent degrees of roughness as a result of their deposition techniques. Deposition can be performed from a number of different copper baths with varying chemistries. The samples were sectioned from circuit board panels and consisted of FR-4 material (glass-filled epoxy) sandwiched between opposing copper layers. In their as-received condition they arrived with an OSP coating (imidazole). Individual test coupons (1 inch x 1 inch) were cut from these panels for testing.

**Optical (Non-Contact) Profilometry.** The first set of etching tests produced samples used for surface roughness evaluation by optical profilometry. Immediately prior to etching, the samples were soaked for 5 minutes in 100% ethanol to remove the imidazole coating. They were then rinsed in deionized water before immersion in the etchant bath.

A surface profile measuring system (WYKO Corporation) was used for non-contact surface profile measurements. The instrument uses white light as the source in an interferometer and measures the degree of fringe modulation or coherence. The instrument is capable of profiling surfaces with root-mean-square roughness ranging from 1 Å to over 20 µm and with steps over 100 µm. Surface area, arithmetic average roughness, root-mean-square roughness, and maximum peak-to-valley measurements are typical outputs available with this technology. ASME 846.1 describes quantitative parameters to characterize surfaces from measured profiles.[31] Parameters are profile-amplitude sensitive, profile-wavelength sensitive, or sensitive to both amplitude and wavelength.

Fourteen samples (seven etching conditions on two substrates) were prepared for non-contact profilometry measurements. Etch times were 60 seconds. Each sample was measured once. Measurement size was approximately 200 µm x 200 µm.

**Wetting Balance.** All copper surfaces intended for solderability tests were cleaned in a standard 10%  $\text{HCl}$  solution for 3 minutes at room temperature. The samples were then rinsed in deionized water before immersion in the etchant bath. These same samples also underwent scanning electron microscopy (SEM) analysis to allow close inspection of resulting surface morphologies to enable correlation between morphology and wettability.

Solder wettability was measured with a commercial wetting balance. This method gives quantitative information on the wetting behavior of solder on a metal substrate under a specific set of conditions. The wetting balance tests were performed with 60Sn-40Pb (wt.%) solder at 245°C. Samples were coated with a rosin, mildly active (RMA) flux and allowed to dry approximately ten minutes prior to wetting balance testing. The immersion times were 10 seconds. The tests used an immersion rate of 20 mm/s and an immersion depth of one mm (approximately 0.04 inches).

Seventy samples (seven etching conditions on two substrates with five replicates) were tested once each for a total of 70 individual wetting balance traces. Etch times were 60 seconds.

**Scanning Electron Microscopy (SEM).** Since only a portion (1 inch x 0.04 inch) of the 1 inch x 1 inch samples were covered with solder at the conclusion of the wetting balance tests, unsoldered areas of these samples were evaluated by SEM to examine their surface morphology. Fourteen samples from Table 3 (seven etching conditions on two substrates) were inspected using SEM.

## Results & Discussion

**Profilometry.** Optical profilometry results for EP and EL copper are shown in Table 3. Path roughness ( $R_p$ ), arithmetic average roughness ( $R_A$ ), root-mean-square roughness ( $R_Q$ ), and maximum peak-to-valley ( $R_T$ ) were calculated for each profile. Since it was difficult to interpret peak-to-valley metrics from EP and EL substrates because of the somewhat rippled surface produced by the underlying laminate layers in the FR-4 substrate, we restrict our discussion to the surface area metric,  $R_p$ . We also believe that  $R_p$  more accurately captures the wettability behavior of these systems based on research showing that the roughness ratio in Wenzel's equation relates to the mean square slope of a surface rather than any measure of amplitude.<sup>[10]</sup> While  $R_p$  is not mean square slope, the two metrics convey similar information. SEM's of representative test surfaces are shown in Figures 1a-1h.

The unetched,  $H_2SO_4/H_2O_2$ , and  $Na_2SO_4/H_2SO_4/H_2O_2$  etched EP copper samples exhibit very similar roughness morphologies (Figure 1a - 1c). The  $R_p$ ,  $R_A$ ,  $R_Q$ , and  $R_T$  metrics are closely grouped for these three conditions. The same trends were seen with the EL copper substrate.

The  $HNO_3/Cu(NO_3)_2$  etched EP copper shows a significant increase over the unetched sample in all four metrics. Not only is surface area increased, but the peak-to-valley dimension (as evidenced by  $R_A$ ,  $R_Q$ , and  $R_T$ ) is increased considerably. An SEM of this substrate is shown in Figure 1d. The  $HNO_3/Cu(NO_3)_2$  etched EL copper shows the same trend with respect to peak-to-valley measurements, but surface area does not appear to be much increased over the unetched sample.

We postulate that the differing morphologies of the EP and EL copper substrates play a role in determining the result of the  $HNO_3/Cu(NO_3)_2$  etch. Perhaps the inherent nature of the EL copper combined with the chemical action of the  $HNO_3/Cu(NO_3)_2$  etch does not promote the roughening required for increased surface area, although it does seem to support the creation/enhancement of large peak-to-valley

distances. Based on these results, one would expect to find large peaks and valleys in the etched EL copper, but with somewhat smooth walls. The etched EP copper, however, should possess the same large peaks and valleys, but with an increased degree of roughening along the walls.

The  $HNO_3/H_2SO_4$  etched EP copper sample appears to be smoother than the unetched EP copper substrate. Not only is the surface area of the etched sample much smaller, but the peak-to-valley dimensions are slightly decreased as well. Apparently, the  $HNO_3/H_2SO_4$  etch effectively smoothes the EP copper surface. The SEM of this substrate, shown in Figure 1e, confirms this observation.

The action of the  $HNO_3/H_2SO_4$  etch on EL copper is not quite as clear. The surface area appears largely unaffected by the etch, but the peak-to-valley metrics are slightly increased. This behavior seems consistent with the  $HNO_3/Cu(NO_3)_2$  etched EL copper, where we postulated that the interaction of the etch with EL copper does not promote the roughening required for increased surface area, although it does seem to support the growth of peak-to-valley distances. Based on these results, one would also expect to find fairly large peaks and valleys in the  $HNO_3/H_2SO_4$  etched EL copper, but again, with somewhat smooth walls.

The  $FeCl_3/HCl$  etch produced the largest roughness gains observed on the EP copper substrate.  $R_p$ ,  $R_A$ ,  $R_Q$ , and  $R_T$  reflect very large increases in surface area and peak-to-valley distances. Figure 1f illustrates the roughened surface. The geometric shapes on the etched surface are a processing side effect to be discussed later. The SEM shown in Figure 1g illustrates the enhanced degree of roughness that can be obtained through increased etching time (90 second etch time).

The  $FeCl_3/HCl$  etch also produced increased surface area on the EL copper, although the effect is not as pronounced. Interestingly, the peak-to-valley metrics are not changed significantly on the EL copper substrate by etching with  $FeCl_3/HCl$ . This behavior is opposite the trend observed with  $HNO_3/Cu(NO_3)_2$  and  $HNO_3/H_2SO_4$  etched EL copper where we postulated that the interaction of the etches with EL copper did not promote the roughening required for increased surface area, although it did seem to support the growth of peak-to-valley distances. Clearly, the  $FeCl_3/HCl$  etch interacts with the EL copper in a different fashion. These observations suggest that some etches do not perform irrespective of substrate, but rather that the etch/substrate pair determines the actual result.

Table 3. Optical profilometry results.

Etch of Interest	EP Copper				EL Copper			
	$R_p$	$R_A$	$R_Q$	$R_T$	$R_p$	$R_A$	$R_Q$	$R_T$
Unetched	1.006314	120	152	1.48	1.017418	316	398	2.92
$H_2SO_4/H_2O_2$	1.005707	139	175	1.57	1.017627	282	355	3.13
$Na_2SO_4/H_2SO_4/H_2O_2$	1.007031	135	172	1.48	1.020976	299	378	3.40
$HNO_3/Cu(NO_3)_2$	1.030769	359	446	3.61	1.019964	461	604	4.59
$HNO_3/H_2SO_4$	1.001754	92	117	1.57	1.016805	375	528	5.05
$FeCl_3/HCl$	1.062241	479	588	3.63	1.026935	310	394	3.08
$CuCl_2/H_2O_2/HCl$	1.045913	256	322	2.58	1.084099	397	498	4.11

60 Second Etch       $R_p$  = Surface Area/Lateral Area ( $\mu m^2/\mu m^2$ )  
20X Magnification       $R_A$  = Arithmetic Average Roughness (nm)

$R_Q$  = RMS Roughness (nm)  
 $R_T$  = Max Peak To Valley ( $\mu m$ )

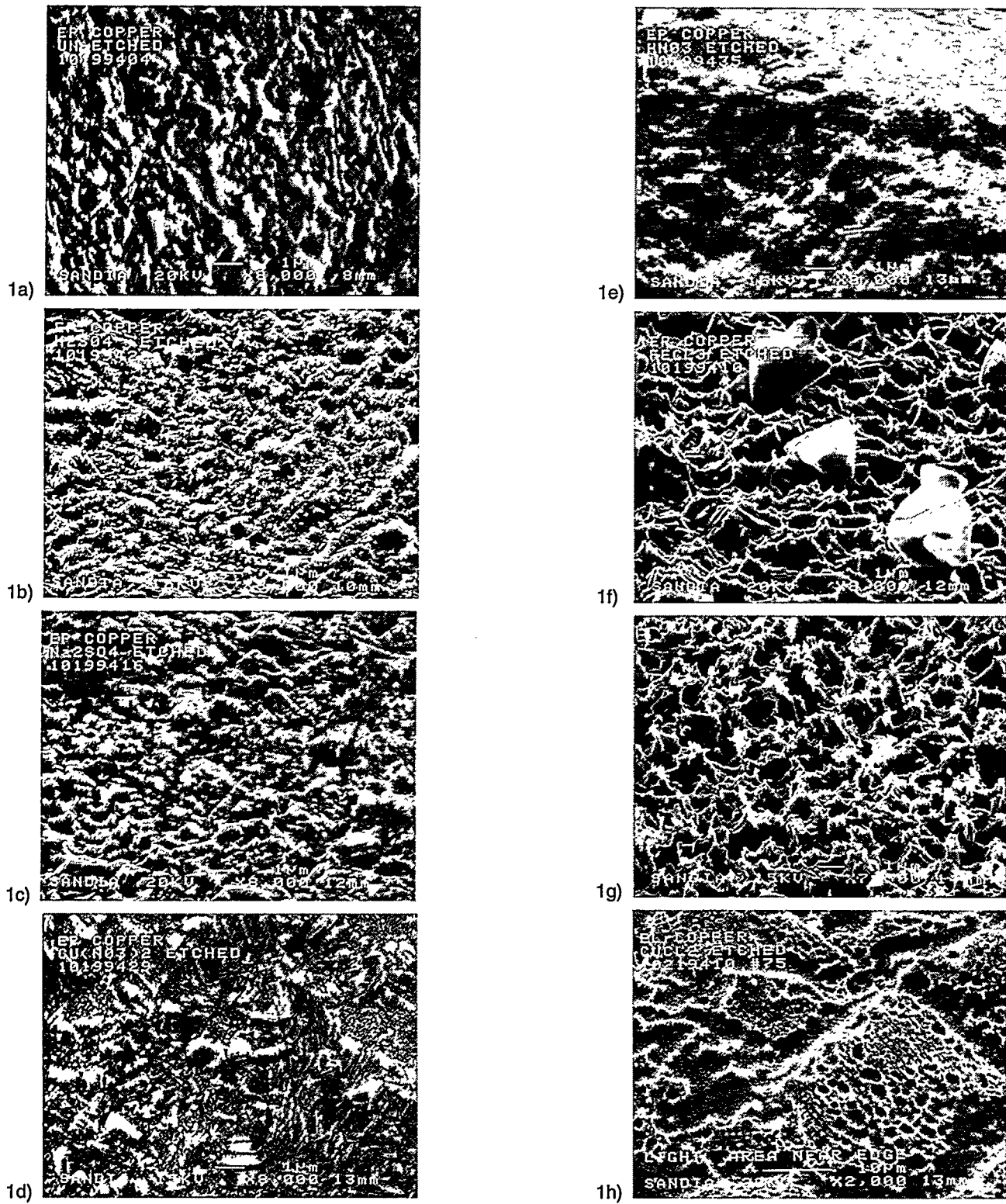


Figure 1. SEM's of test surfaces. 60 sec etches and EP copper substrates except as noted. Micrographs a - f at 8000X magnification with 1  $\mu$ m fiduciary marks. Micrograph g at 7500X mag with 1  $\mu$ m fiduciary mark. Micrograph h at 2000X mag with 10  $\mu$ m fiduciary mark. a) Unetched b)  $H_2SO_4/H_2O_2$  c)  $Na_2SO_4/H_2SO_4/H_2O_2$  d)  $HNO_3/Cu(NO_3)_2$  e)  $HNO_3/H_2SO_4$  f)  $FeCl_3/HCl$  g)  $FeCl_3/HCl$  (90 sec) h)  $CuCl_2/H_2O_2/HCl$  (EL Cu)

The  $\text{CuCl}_2/\text{H}_2\text{O}_2/\text{HCl}$  etch was the final condition to be evaluated. In many ways it was the most successful in producing the roughness morphology that we believed would enhance wettability/solderability. Considerable gains in roughness were achieved on EP and EL copper substrates with the  $\text{CuCl}_2/\text{H}_2\text{O}_2/\text{HCl}$  etch. As shown in Table 3, surface area (as evidenced by  $R_p$ ) and peak-to-valley height (as evidenced by  $R_A$ ,  $R_Q$ , and  $R_T$ ) are significantly increased over the unetched state on both EP and EL copper. The SEM in Figure 1h illustrates the roughened surface that was obtained using the  $\text{CuCl}_2/\text{H}_2\text{O}_2/\text{HCl}$  etch. This SEM photo, taken on EL instead of EP substrate, clearly shows the presence of grooves on the etched surface. The etch appears to preferentially attack the grain boundaries of the columnar EL copper structure and also roughen the grains on a finer scale. EP samples also possessed this topology. Selective dissolution of grain boundaries is a well-known phenomenon that is often used in metallography to achieve visualization of grain boundaries.[32]. To appreciate the size of the grooves, notice that the magnification of Figure 1h is approximately four times smaller than in Figures 1a-1g.

**Solderability.** Wetting balance experiments with the  $\text{H}_2\text{SO}_4/\text{H}_2\text{O}_2$ ,  $\text{Na}_2\text{SO}_4/\text{H}_2\text{SO}_4/\text{H}_2\text{O}_2$ ,  $\text{HNO}_3/\text{Cu}(\text{NO}_3)_2$ , and  $\text{HNO}_3/\text{H}_2\text{SO}_4$  etches demonstrated that no measurable solderability gains were achieved on EP or EL copper with these solutions. This is in agreement with the profilometry results and SEM's which showed no significant roughening from the three  $\text{H}_2\text{SO}_4$ -containing etches. The exception to roughening is the  $\text{HNO}_3/\text{Cu}(\text{NO}_3)_2$  etch, which produced increased  $R_A$ ,  $R_Q$ , and  $R_T$  in both EP and EL substrates. In the EP  $\text{HNO}_3/\text{Cu}(\text{NO}_3)_2$  case,  $R_p$  was also increased. Apparently, the increased surface area produced by the  $\text{HNO}_3/\text{Cu}(\text{NO}_3)_2$  etch did not translate into increased wettability/solderability. Perhaps the degree of roughness was insufficient to affect solderability. It is also possible that some surface morphologies leading to increased surface area are not conducive to increased solder flow. The major features on the surface of the EP sample etched in  $\text{HNO}_3/\text{Cu}(\text{NO}_3)_2$ , shown in Figure 1d, are stacked, faceted protrusions with sheer faces. Rod-like fibril shapes are interspersed across the surface. There appears to be no connecting pathways or vias to promote or sustain solder flow. In fact, in many areas the solder flow could actually be impeded by the protrusions.

The morphologies of the unetched,  $\text{H}_2\text{SO}_4/\text{H}_2\text{O}_2$ , and  $\text{Na}_2\text{SO}_4/\text{H}_2\text{SO}_4/\text{H}_2\text{O}_2$  etched samples are nearly indistinguishable (Figures 1a-1c). Very little roughening was introduced with these two etches so we would not expect any major roughness-based improvements in solderability.

The smooth non-homogeneous surface produced by the  $\text{HNO}_3/\text{H}_2\text{SO}_4$  etch (Figure 1e) is not the type of morphology we would expect to produce wettability improvements. With  $R_p$  values below their unetched counterparts, both EP and EL  $\text{HNO}_3/\text{H}_2\text{SO}_4$  etched substrates held little promise for solderability gains. This prediction was borne out in wetting balance tests. In fact, wettability was poorer on the etched EL surface than on the unetched condition. An oxide detected by SEM/EDS could have been a contributory factor in the poor performance of the etched EL sample. The strongly oxidizing nature of the  $\text{HNO}_3/\text{H}_2\text{SO}_4$  etching bath could be responsible for the oxide signature on the surface.

The very large  $R_p$  value of the  $\text{FeCl}_3/\text{HCl}$  etch on EP copper (1.062241 compared to the unetched condition of 1.006314) was a promising indicator of potential wettability improvements. Figure 2 plots wetting balance results for the  $\text{FeCl}_3/\text{HCl}$  etch vs. the unetched condition on EL copper. Qualitatively, they are difficult to distinguish. Inspection of the full data set shows that some of the  $\text{FeCl}_3/\text{HCl}$  etched samples attained a higher wetting force and produced a greater wetting rate than their unetched counterparts, but it is unclear if these differences are significant.

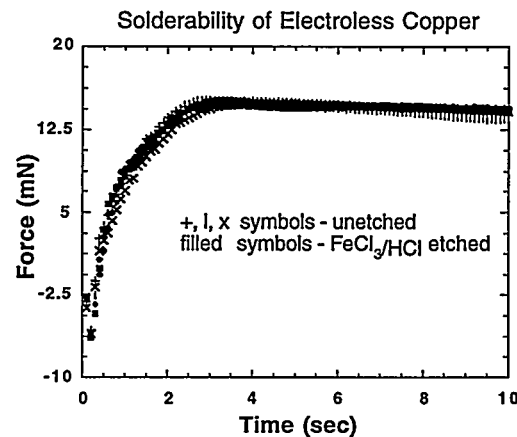


Figure 2. Wetting balance results for the unetched and  $\text{FeCl}_3/\text{HCl}$  etched conditions on EL copper. Three samples are shown for each condition.

The true performance of the  $\text{FeCl}_3/\text{HCl}$  etch was likely underestimated because the etched samples were not ideally processed. SEM/EDS analysis detected a chlorine presence on the surface of the  $\text{H}_2\text{O}$  rinsed  $\text{FeCl}_3/\text{HCl}$  etched samples. As shown in Figure 1f,  $\text{CuCl}$  (nantokite) crystals, as identified by X-ray diffraction, were scattered on the surface. The presence of these crystals was a side effect of our etching process. While the nantokite crystals did not cover a large portion of the surface, their presence was reflected in the wetting balance results.

Wetting balance results for the  $\text{CuCl}_2/\text{H}_2\text{O}_2/\text{HCl}$  etch were originally poor. In this instance, SEM/EDS analysis detected a significant chlorine presence on the surface of the  $\text{CuCl}_2/\text{H}_2\text{O}_2/\text{HCl}$  etched samples. The entire surface appeared to be coated with crystalline bodies conformal to an underlying channelled topography. X-ray diffraction again identified the species as nantokite. As all etches were concluded with a deionized  $\text{H}_2\text{O}$  rinse, we theorized that the nantokite presence was a result of the interaction between the copper removed from the surface and the  $\text{H}_2\text{O}$  rinse.

If this dragout/quenching were to produce a nantokite layer on the surface, no subsequent amount of  $\text{H}_2\text{O}$  rinsing would remove the layer since nantokite has a very low solubility in  $\text{H}_2\text{O}$  (.0062 g/100 cc). Nantokite is, however, soluble in  $\text{HCl}$ . Since copper is only very slightly soluble in  $\text{HCl}$ , we re-ran the  $\text{CuCl}_2/\text{H}_2\text{O}_2/\text{HCl}$  etch using an  $\text{HCl}$  rinse in place of the  $\text{H}_2\text{O}$  rinse. We expected that the  $\text{HCl}$  rinse would not alter the morphology created by the  $\text{CuCl}_2/\text{H}_2\text{O}_2/\text{HCl}$  etch. As a result of this processing

change, we were able to achieve wetting balance results similar to the  $\text{FeCl}_3/\text{HCl}$  etch. However, it is difficult to capture the improvement with the wetting balance alone.

Figures 3a and 3b show optical micrographs of the soldered unetched sample and soldered  $\text{CuCl}_2/\text{H}_2\text{O}_2/\text{HCl}$  etched sample, respectively. In Figure 3c, an enlargement of Figure 3b, the etched sample exhibited solder branching not seen on the unetched substrate. Solder was aggressively wetting the surface. Dendritic fingers have spread in advance of the bulk. This behavior could be related to the precursor foot (i. e. Sn-rich front) observed by others.<sup>[33-35]</sup> The  $\text{CuCl}_2/\text{H}_2\text{O}_2/\text{HCl}$  solution was the only etch that exhibited this behavior.

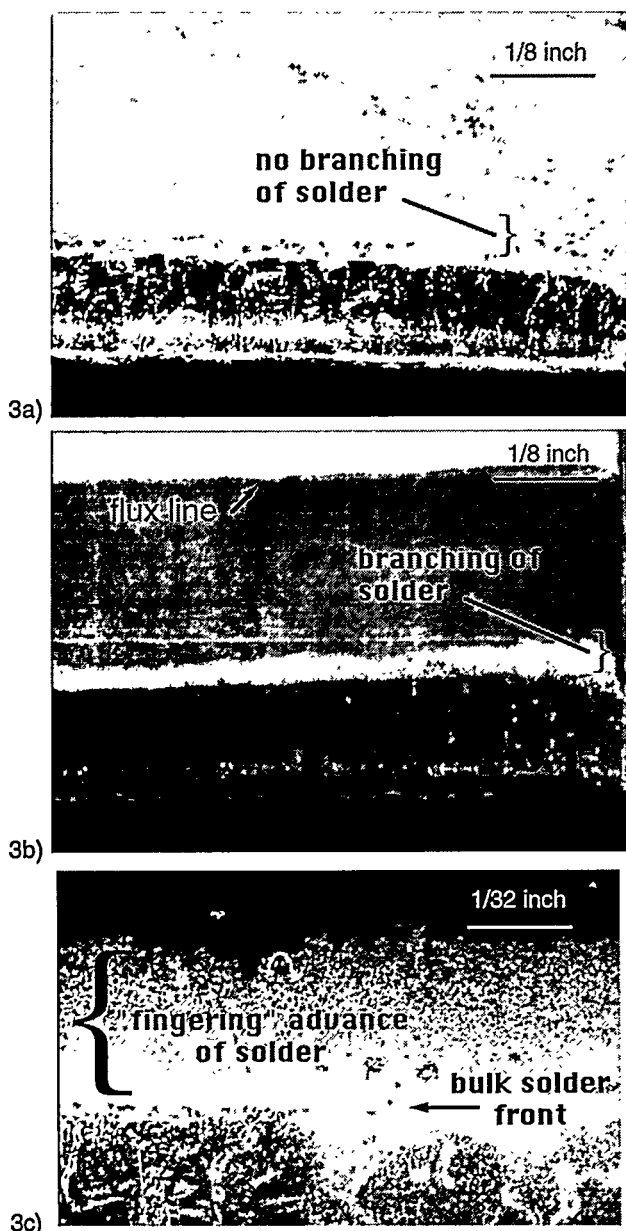


Figure 3. Optical micrographs of soldered samples.  
a) Unetched b)  $\text{CuCl}_2/\text{H}_2\text{O}_2/\text{HCl}$  etched c) Enlargement of b at solder front

Figure 4 contrasts the surface morphology of the unetched and  $\text{CuCl}_2/\text{H}_2\text{O}_2/\text{HCl}$  etched sample. In Figures 4b and 4c, the etched substrate has a matrix of deep, interconnected grooves spanning the surface. The unetched sample in Figure 4a shows the typical nodular morphology of EL copper deposits. Figure 5 contrasts unetched,  $\text{FeCl}_3/\text{HCl}$  etched, and  $\text{CuCl}_2/\text{H}_2\text{O}_2/\text{HCl}$  etched surfaces at higher magnifications. The  $\text{FeCl}_3/\text{HCl}$  etch produces uniform small scale roughness, but does not produce V-shaped grooves. The  $\text{CuCl}_2/\text{H}_2\text{O}_2/\text{HCl}$  etch not only produces small scale roughness, but also deep V-shaped grooves ideal for capillary flow of solder.

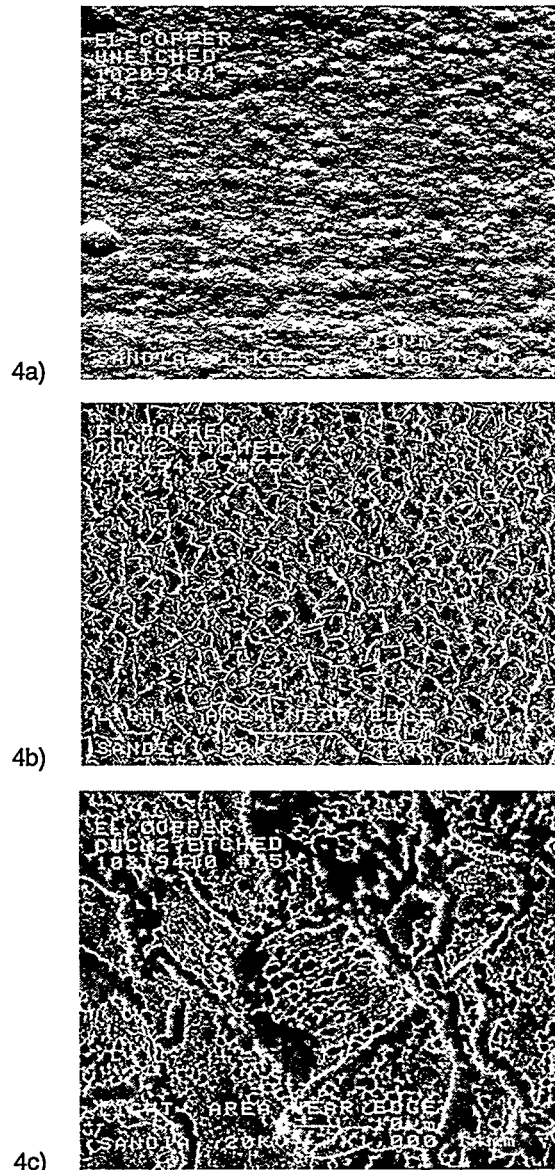


Figure 4. SEM's of EL copper test surfaces at low magnification. a) Unetched - 500X mag with 10  $\mu\text{m}$  fiducial mark b)  $\text{CuCl}_2/\text{H}_2\text{O}_2/\text{HCl}$  etched - 200X mag with 100  $\mu\text{m}$  fiducial mark c) Enlargement of b - 1000X mag with 10  $\mu\text{m}$  fiducial mark

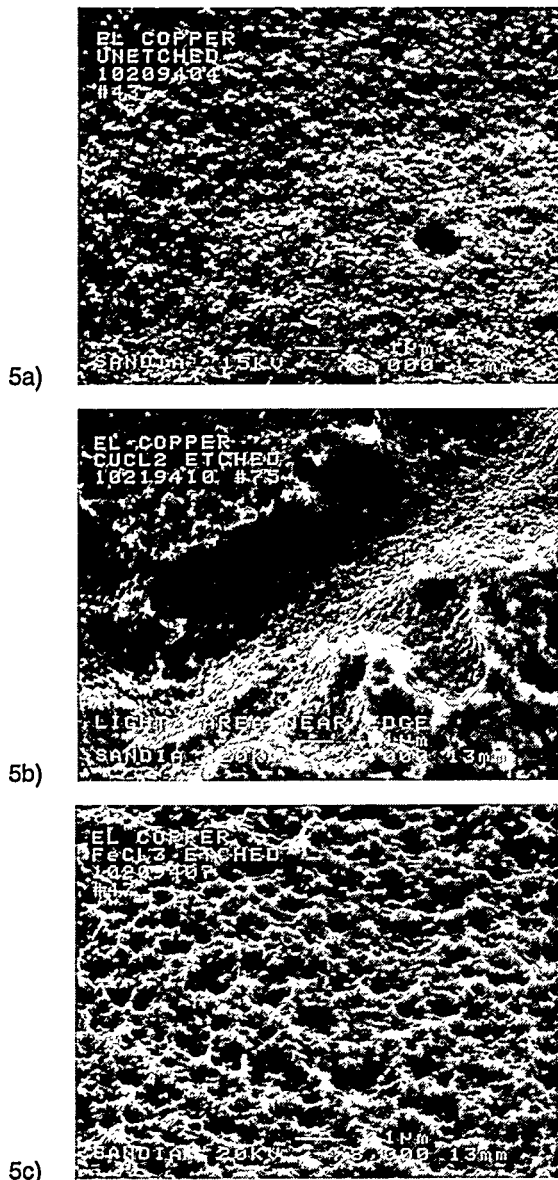


Figure 5. SEM's of EL copper test surfaces at high magnification. All three micrographs at 8000X magnification with 1  $\mu$ m fiduciary marks. a) Unetched b)  $\text{CuCl}_2/\text{H}_2\text{O}_2/\text{HCl}$  etched c)  $\text{FeCl}_3/\text{HCl}$  etched

These encouraging results with  $\text{FeCl}_3/\text{HCl}$  and  $\text{CuCl}_2/\text{H}_2\text{O}_2/\text{HCl}$  on FR-4 led us to conduct an additional solder wetting and flow experiment on a Ball Grid Array Test Vehicle (BGATV). The BGATV is a series of EP copper pads and lines of various sizes and widths deposited on a circuit board. A small subsection of the BGATV is shown in Figure 6. 63Sn-37Pb (wt.%) solder paste is stenciled onto the round pad areas in Figure 6 and RMA flux is brushed onto the exposed copper surfaces. The BGATV is then passed through a solder reflow machine ( $\text{N}_2$  cover) at 9 inches per minute where a series of hot plates melt the solder paste in a controlled manner. The objective is to induce solder flow down the lines from the pads, completely filling the interior of each pattern.

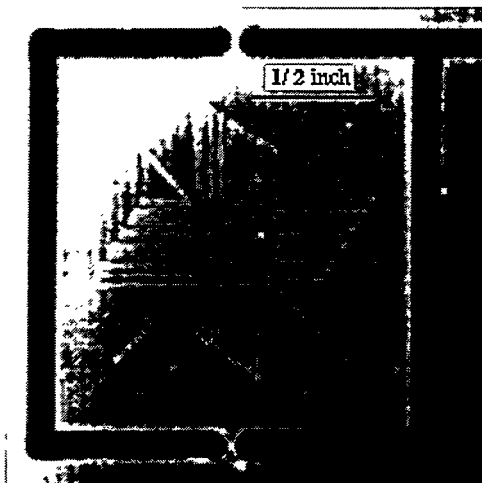


Figure 6. Copper-patterned area of a BGATV.

Experiments with unetched BGATV's have been only partially successful in realizing the goal of complete solder coverage. Wide lines ( $> 20$  mils) have successfully conveyed the solder. Finer lines ( $< 20$  mils), however, have not supported solder flow. The effects of etching on wettability can be determined by etching the BGATV's with  $\text{FeCl}_3/\text{HCl}$  and  $\text{CuCl}_2/\text{H}_2\text{O}_2/\text{HCl}$  and measuring solder flow. Figure 7 shows the results of these initial measurements. Etching appears to improve wettability down the lines. Although each of the three cases contained poor performing lines, the unetched BGATV's had many lines that did not wet. There were many fewer lines on the etched BGATV's that did not exhibit some degree of wetting. Optical profilometry measurements performed prior to BGATV wettability testing capture the enhanced roughness produced by etching (Table 4). Measurements were made on three areas of the BGATV. The etching appears non-uniform as evidenced by rather large standard deviations in the roughness measurements. This non-homogeneity in etching may also explain the large standard deviations observed in the solder flow measurements.

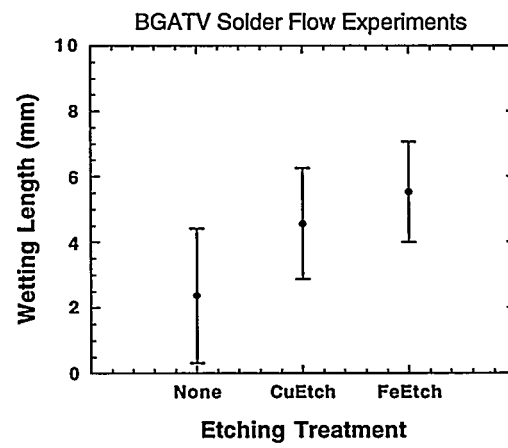


Figure 7. Results of solder flow experiments on BGATV's.

Table 4. Optical profilometry measurements of BGATV's.

Etching Treatment	Surface Area Index (i. e. $R_p$ )		
	Area 1	Area 2	Area 3
Unetched	1.87±0.10	1.91±0.10	1.84±0.07
FeCl <sub>3</sub> /HCl	2.83±0.02	3.37±0.50	3.27±0.46
CuCl <sub>2</sub> /H <sub>2</sub> O <sub>2</sub> /HCl	2.54±0.30	2.69±0.40	2.38±0.41

60 Second Etch      80X Magnification

$R_p$  = Surface Area/Lateral Area ( $\mu\text{m}^2/\mu\text{m}^2$ )

## Summary

We produced physically rougher surfaces through chemical etching of electroplated and electroless-plated copper on FR-4 laminate board. Roughnesses were characterized using optical interferometry and SEM. One of the etches (CuCl<sub>2</sub>/H<sub>2</sub>O<sub>2</sub>/HCl) produced a grooved topography and demonstrated very good wetting behavior, perhaps exceeding the FeCl<sub>3</sub>/HCl etch patented by Rockwell. We have further tested the FeCl<sub>3</sub>/HCl and CuCl<sub>2</sub>/H<sub>2</sub>O<sub>2</sub>/HCl etchants on a Ball Grid Array Test Vehicle device board to determine real-world applicability. Noticeable improvements in wettability/solderability were observed through chemical etching of copper substrates.

## Acknowledgments

The authors wish to thank Dr. Ken Meissner for his critical review of this manuscript. The authors acknowledge Cindy Hernandez, Gary Zender, and Mary Gonzales for the wetting balance experiments, SEM, and XRD, respectively. Barry Ritchey and Celeste Drewien contributed SEM expertise. We thank Melanie Romero for sample preparation, Dipesh Goel for assistance with SEM photos, George Wenger of AT&T for supplying the PWB's, and the NCMS Surface Finishes Team for their input into the experimental study. This work was performed at Sandia National Laboratories in collaboration with the National Center for Manufacturing Sciences under CRADA CR91/1030 supported by the U.S. Department of Energy under contract DE-AC04-94AL85000.

## References

1. R. N. Wenzel, *Ind. Eng. Chem.* **28**, 988 (1936).
2. E. R. Parker and R. Smoluchowski, *Trans. ASM* **35**, 362 (1944).
3. R. Shuttleworth and G. L. J. Bailey, *Disc. Faraday Soc.* **3**, 16 (1948).
4. Y. V. Goryunov, *Russ. Chem. Rev.* **33**, 467 (1964).
5. R. E. Johnson and R. H. Dettre, *Contact Angle, Wettability, and Adhesion* (edited by R. F. Gould), Advances in Chemistry Series 43, American Chemical Society, Washington, D.C. (1964).
6. S. J. Hitchcock, N. T. Carroll, and M. G. Nicholas, *J. Mater. Sci.* **16**, 714 (1981).
7. M. G. Nicholas and R. M. Crispin, *J. Mater. Sci.* **21**, 522 (1986).
8. A. M. Cazabat and M. A. Cohen Stuart, *J. Phys. Chem.* **90**, 5845 (1986).
9. L. Romero and F. G. Yost, *J. Fluid Mech.* Submitted.
10. F. G. Yost, J. R. Michael, and E. T. Eisenmann, *Acta Metall. Mater.* **43**, 299 (1995).
11. D. M. Tench and D. P. Anderson, "Uniform Solder Coating on Roughened Substrate", Rockwell International Corp., US Patent 5178965 (1993).
12. N. R. Sorensen and F. M. Hosking, "Solderability Preservation Through the Use of Organic Inhibitors", *Conference Proceedings of Interpack 95*, Maui, HI (March 1995).
13. N. J. Nelson, "Process and Structure for Etching Copper", PSI Star Inc., US Patent 4451327 (1984).
14. E. B. King, "Continuous Redox Process for Dissolving Copper from Substrates", Southern California Chemical Co. Inc., US Patent 3705061 (1972).
15. "Diffusion Bonding of Copper to Ceramic Substrates for Semiconductor Module", Tokyo Shibaura Dauki KK, European Patent 115158-A2 (1984).
16. J. Ling and C. E. Albright, "The Influence of Atmospheric Contamination on Copper to Copper Ultrasonic Cleaning", *Proceedings of 34th Electronics Components Conference*, CHMT/EIA Conference, New Orleans, LA, IEEE, 84CH2030-5, 209-218 (1984).
17. E. Kauzor, "Preparation of Test Pieces for Macroscopic Examination", *Praktiker*, **30**, 5 82-84 (May 1978).
18. J. T. Moore, "Continuous Ammoniacal Etches", *Electroplat. Met. Finish.*, **29**(5), 6-8 (1976).
19. S. J. Beyer and R. M. Lukes, "Regeneration of Ferric Chloride Copper Etching Solutions", General Electric Co., US Patent 3794571 (1974).
20. M. A. Douglas, "Copper Dry Etch Process Using Organic and Amine Radicals", Texas Instruments, US Patent 5100499 (1992).
21. A. Caruana and H. Rainer, "Process for Etching Work Pieces Using Copper Tetramine Complex", DuPont E. I. de Nemours and Co., US Patent 5076885 (1991).
22. A. J. Brock and M. J. Pryor, "Process for Etching Copper Base Materials Using Peroxydisulfuric Acid and Halide", Olin Corp., US Patent 4973380 (1990).
23. P. A. Martens and N. J. Nelson, "Copper Etching Process and Product with Controlled Nitrous Acid Reaction", PSI Star Inc., US Patent 4927700 (1990).
24. D. J. Barnett, J. F. Battey, and N. J. Nelson, "Copper Etching Process and Product Using Liquid Etchant", PSI Star Inc., US Patent 4767662 (1988).
25. N. J. Nelson, "Copper Etching Process and Solution", PSI Star Inc., US Patent 4632727 (1986).
26. W. M. McGowan, "Solution and Process for Treating Copper and Copper Alloys", Lea Manuf. Co., US Patent 4510018 (1985).
27. I. Katsutoshi and M. Akira, "Etching Solutions for Copper and Copper Alloys", Tokai Electrochemical Co., US Patent 3939089 and US Patent 3936332 (1976).
28. E. Winfried and R. Alfred, "Process and Apparatus for Etching Copper and Copper Alloys", Hoellmueller Hans Maschinebau, US Patent 3880685 (1975).
29. N. J. Nelson, "Process for Etching an Aluminum-Copper Alloy with Chlorine", PSI Star Inc., US Patent 4468284 (1984).
30. J. Chiang, "Process of Etching Copper Circuits", FMC Corp., US Patent 3844857 and US Patent 3837945 (1974).
31. ASME 846.1 85, American Society of Mechanical Engineers (1992).
32. V. E. Fradkov, *Scripta Metall. et Mat.*, **30**(12), 1599-1603 (1994).
33. A. Bondi, *Chem. Rev.* **52**, 417 (1953).
34. G. C. Smith and C. Lea, *Surf. Inter. Analy.* **9**, 145 (1986).
35. T. J. Singler, J. A. Clum, and E. R. Prack, *Trans. ASME*, **114**, 128 (1992).